Review Article

Advances in neuro-oncological imaging and their impact on patient management

Arsany Hakim, Roland Wiest

Department of Neuroradiology, University Institute of Diagnostic and Interventional Neuroradiology, Inselspital, University of Bern, Bern, Switzerland

Abstract

Neuroradiological imaging of gliomas has undergone many advances in the recent years. Visual assessment of structural image datasets is nowadays complemented by quantifiable imaging markers to detect tumor progression and correlations with molecular markers. Detailed information about the tumor-specific pathophysiology, reflected by alterations of hemodynamics and metabolism or about tumor microstructure and infiltration of neighboring structures, is nowadays accessible noninvasively through the magnetic resonance imaging (MRI). Some of these developments have been driven by the updates of the neuropathological classification of gliomas, which now ranks genotypic markers ahead of histomorphological criteria. Neuroimaging constitutes also a key element in the diagnostic support, therapy planning, and monitoring of disease progression under therapy. While computed tomography is still of importance in emergency situations to screen for neoplastic cerebral lesions or acute complications of therapy or tumor progression, as for example, hemorrhage or seizure generation, MRI is the fundamental technology for the differential diagnosis and localization of cerebral gliomas. This review aims at providing an introduction into the most frequent clinically employed advanced magnetic resonance methods for glioma imaging.

Keywords: Genetic status of brain tumours, glioma, imaging markers, magnetic resonance sequences

Address for correspondence: Prof. Roland Wiest, University Institute of Diagnostic and Interventional Neuroradiology, Inselspital, University of Bern, 3010 Bern, Switzerland.
E-mail: roland.wiest@insel.ch
Published: 02-11-2021

INTRODUCTION

Magnetic resonance imaging (MRI) provides important information about the diagnosis and the biological plausibility of imaging features to reflect the molecular differences of different tumor categories [Table 1] and the most important differential diagnoses as brain abscess, lymphoma, or metastasis. However, MRI examinations still vary considerably in terms of field strength, magnetic resonance (MR) protocols, MR sequence design, scanner type, slice thickness, and image contrast. Therefore, examination protocols require further standardization with minimum requirements encompassing high-resolution Fluid attenuated inversion recovery (FLAIR) and KM-based 3-D T1-weighted sequences in addition to native T1- and T2-weighted sequences and follow-up at similar field strengths (EORTC and NBTS recommendations for structural MRI).[1] The integration of 3-D T1-weighted sequences plays a particularly important role for quantitative volumetric determination of tumor geometry and tumor progression and the application of RANO criteria.[2] Limitations of conventional MRI and qualitative assessment of therapy response include a low sensitivity to distinguish between

Access this article online	
Quick Response Code:	Website: www.internationaljneurooncology.com
	DOI: 10.4103/IJNO.IJNO_403_21

How to cite this article: Hakim A, Wiest R. Advances in neuro-oncological imaging and their impact on patient management. Int J Neurooncol 2021;4:S16-26.

Table 1: Tumor classification: Imaging markers according to genetic status

Genetic status	Imaging characteristics
1p/19q co-deletion (oligodendroglioma)	Frontal-, parietal- and occipital lobe Indistinct tumor margins Heterogeneous T2-signal Calcification Perfusion increase (rCBV) Increased glucose metabolism (FDG-PET)
1p/19q intact (diffuse astrocytoma)	Temporal lobe/insula Distinct margins Homogenous signal on T1w and T2 images rCBV not elevated in Grade II gliomas
IDH mutation (GII, GIII, secondary GBM)	Periventricular and subventricular zone/frontal lobe Distinct margins Homogeneous signal Large portions of unenhanced tumors Cyst and small satellites
IDH intact (wild type)	2 Hydroxyglutarate peak (MR spectroscopy) Multilobar tumor, fronto-temporo-insular predilection rCBV elevated Increased APT-weighted CEST signal
MGMT promotor methylated GBM	Temporal-, parietal- or occipital lobe Edema less pronounced Nodular contrast enhancement Lower rCBV Lower rCBF Increased permeability
MGMT promotor unmethylated GBM	Temporal lobe, basal ganglia, subventricular zone Ring-enhancement Pronounced edema Elevated rCBV Lower permeability

GBM: Glioblastoma, rCBV: Relative cerebral blood volume, MR: Magnetic resonance, CEST: Chemical exchange saturation transfer, APT: Amide proton transfer, rCBF: Regional cerebral blood flow, IDH: Isocitrate dehydrogenase, MGMT: Methylation of O6-methylguanine DNA methyl transferase

true tumor progression and therapy-induced effects and investigator-dependent biases.[3] In this regard, the applications of advanced neuroimaging methods for tissue typing such as MR spectroscopy (MRS), perfusion or diffusion imaging offer higher sensitivity and specificity but are hardly standardized compared to standard protocols. In a survey of a total of 220 centers in Europe, 85% of the centers surveyed stated that they had implemented perfusion imaging as a standard in glioma protocols, whereas MRS, although available in approximately 80% of the centers, is frequently used on an individual basis for specific indications.[4] For presurgical planning of gliomas that are located in eloquent areas of the brain, functional imaging techniques in combination with diffusion tractography are nowadays routine in most centers. In this review, we provide an overview on advanced imaging techniques that aid in the differential diagnosis and follow-up of gliomas.

Perfusion imaging

Perfusion imaging has become a core element of advanced imaging protocols in the assessment of gliomas due to the ability to investigate the vasculature and permeability of brain tumor tissue. Measuring the microvascular circulation on MRI is either based on an exogenous tracer (contrast agent) or an endogenous tracer (contrast-free). Using gadolinium chelates as a tracer, perfusion imaging is either based on T2* effects (dynamic susceptibility contrast, DSC) or T1-weighted (dynamic contrast-enhanced, DCE) methods.

Dynamic contrast-enhanced perfusion imaging

DCE measures the shortening of T1 relaxation time when gadolinium passes through the brain tissue estimating the extravasation of contrast from the intravascular space to the extracellular space. DCE perfusion offers advantages in terms of quantifying blood–brain barrier disruption of gliomas as a marker of histopathologic malignancy grade, and DCE requires complex pharmacokinetic modeling. One of the most important advantages of the DCE is its robustness against susceptibility artifacts that are caused by postoperative material or blood products compared to T2*-based methods.[5] Using postprocessing techniques, several parameters can be calculated. These parameters reflect hemodynamic features of the region under investigation. In addition, pharmacokinetic models[6-8] evaluate the transfer of the volume of tracer between the intravascular space (i.e., plasma) and the extravascular extracellular space and the underlying tumor vasculature.

In DCE perfusion, several parameters can be used to evaluate the microvascularity of the tumor bed: (i) the area under the curve (AUC), (ii) initial AUC, (iii) K_{trans} (volume transfer constant between blood plasma and extravascular extracellular space), (iv) the v_e (extravascular extracellular volume fraction), (v) v_p (blood plasma volume), (vi) k_{ep} (reverse transfer constant, (vii) wash-in, and (viii) wash-out rates.[9,10]

Dynamic susceptibility contrast perfusion imaging

DSC is based on a susceptibility-induced signal loss on T2*-weighted sequences by the bolus passage of gadolinium through the microvasculature of the brain. DSC perfusion offers advantages in terms of detecting cerebral blood flow (CBF) and transit time of the contrast bolus in the tumor and its surrounding edema[5] For DSC perfusion, the most frequently used postprocessing technique is the deconvolution method (to estimate the tissue residue function by removing the contribution from the arterial input function). In DSC, different perfusion parameter can be calculated, as e.g., cerebral blood volume (CBV), CBF, permeability and various parameters of the transit time of the contrast passage. In brain tumors, the most important parameters used in DSC perfusion are the K2 (permeability map) which is the leakage coefficient calculated by linear fitting of the T2* signal intensity

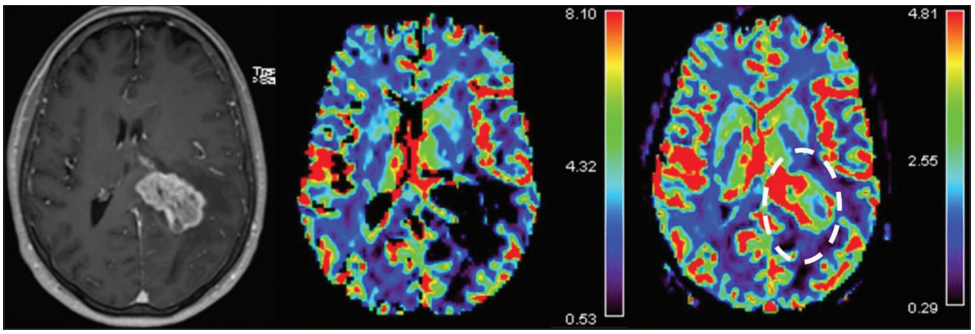

Figure 1: Leakage correction in a patient with left sided high-grade glioma (left). Hyperperfusion is absent in the cerebral blood volume map without leakage correction (middle), while detectable in the cerebral blood volume map with mandatory leakage correction (circle, right image)

curve,[10] and the corrected CBV [Figure 1]. As contrast pooling due to leakage through the blood–brain barrier causes T1 shortening, the time concentration curve decreases below the baseline, hence corrections for this effect are important for glioma imaging. Corrections can be performed by optimizing the scanner parameters (such as using a lower flip angle to minimize the T1 effect),[11] preloading with Gadolinium to partially saturate the baseline T1 signal contribution,[12-14] or via postprocessing by using one of different available mathematical models (such as the Boxerman-Schmainda-Weisskoff linear fitting algorithm)[15,16] as well as by various combinations of these methods.[17] Some authors also recommend peak height and percentage of signal recovery analysis.[9]

Perfusion analysis is useful in evaluating tumor vascular pathology, since it provides information about tumor entity, grading, and to some extent the molecular fingerprints. A hallmark of aggressive and infiltrative tumors are immature endothelial cells with loose junctions and proliferative and invasive cells, irregular, and tortuous vessels or arteriovenous shunts. Low-grade gliomas are composed of normal endothelial cells with relatively intact blood-brain barrier.[10,18] CBV is a marker of microvascular density[19,20] and it informs about tumor vascularity (neoangiogenesis), which is an important feature in high-grade gliomas. The permeability surface area product is a marker for microvascular cellular proliferation,[21] since increasing angiogenic activity of immature vascular structures result in "leaky" vessels.[5] In clinical routine, quantitative analysis is performed by drawing a region of interest into the suspected lesion (contrast-enhancing lesions and peritumoral region). The measurements within the tumor region are compared with areas within the normal-appearing white matter [Figure 2]. However, to find the right threshold to differentiate between different entities (e.g., tumor recurrence and radiotherapy or different grades of tumors) is challenging. Ratios differ in their cutoff values and technical factors affect thresholding. Imaging

Figure 2: Quantitative analysis of dynamic susceptibility contrast perfusion by delineation of a region of interest. In a patient with left frontal Grade IV glioma, the time intensity curves indicate the differences in the time attenuation curves within the glioma and the reference region in the unaffected hemisphere

protocols and sequence parameters, bolus preloading, and postprocessing methods are subject to confounders.[17,22]

Recent methods to detect microcirculation without the need of contrast injection, such as the so-called intravoxel incoherent motion perfusion or arterial spin labeling allow the detection of regional blood flow changes in tumor tissue without contrast agent application, but are still mostly used in the context of studies to predict therapy response and for tumor grading.[23,24]

Magnetic resonance spectroscopy

Isocitrate dehydrogenase (IDH) status and 1p/19q codeletion are the important aspects of modern tumor classification and thus essential for preoperative workup. Therefore, noninvasive consideration of genetic imaging markers is of great relevance. IDH mutations are involved in glioma genesis and are present in most Grade 2 and 3 gliomas and in secondary glioblastomas (GBM).[25] Oligodendroglial tumors are classified based on 1p/19q codeletion. Frontal and parietal predilection, indistinct tumor margins or calcifications in the 1p/19q codeleted gliomas compared to temporal or insular predilection and more homogeneous signal intensities of the tumor matrix in diffuse gliomas allow a first estimation of the underlying tumor entity with conventional MRI [Table 1].[26-29] In gliomas, proton (1H) MRS provides a spectrum of pathological brain metabolites encompassing

elevated creatine and choline (reflecting cell proliferation) and decreased N-acetylaspartate (NAA) (loss of neuronal integrity). Increased myoinositol levels favor the diagnosis of low grade gliomas and elevated lactate points toward higher grade gliomas [Figure 3].

MRS enables the delineation between different tumor grades and supports differential diagnosis of inflammatory or infectious central nervous system diseases. Further, it allows the identification of genetic markers by the detection of 2-hydroxglutarate[30] in IDH-mutated tumors.[31-33] MRS enables tracking of molecules related to tumor grade and tissue invasion and has been shown to be superior to conventional imaging markers, perfusion imaging, and diffusion imaging in differentiating IDH wild type from IDH-mutated gliomas [Figure 4].[26,34]

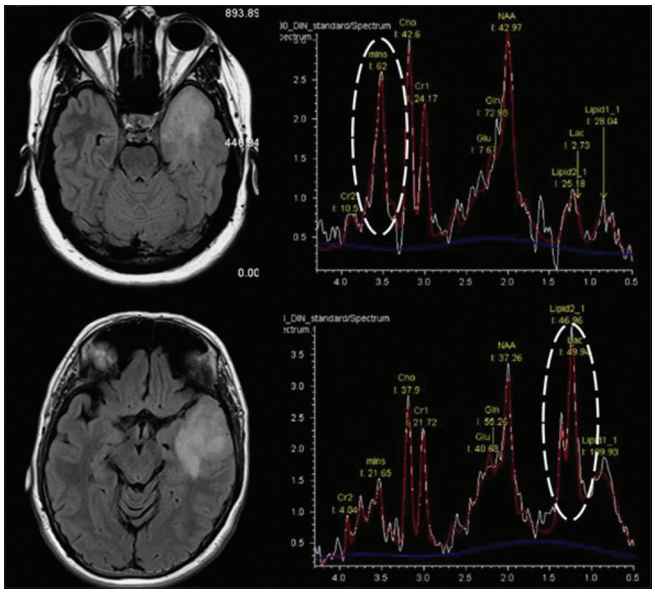

Figure 3: Magnetic resonance spectroscopy of two patients with left temporal gliomas. The images in the upper row display a histologically proven low-grade glioma. The magnetic resonance spectroscopy denotes an increased myo-inositol peak at 3.5ppm as a marker for a low grade glioma. The images in the lower row display a histologically proven Grade IV glioma. The magnetic resonance spectroscopy shows a lipid peak resonating at 1.3 ppm due to release of membrane lipids as a marker for tissue infiltration and damage

Chemical exchange saturation transfer (imaging)

Amide proton transfer (APT)-weighted imaging (chemical exchange saturation transfer, CEST) is an MRI technique whose image contrast is based on chemical exchange between hydrogen atoms and mobile protons in amides, amines, and hydroxyl groups.[35,36] The signal from the protons of peptide chains in proteins is too low to be measured by normal MRI. The exchange between protein amide groups and surrounding water opens a possibility to measure these protons. In tumor regions, the concentration of proteins is elevated compared to surrounding tissues, and subsequently, the increased intracellular exchanges lead to an increased APT level [Figure 5]. Applications for APT-CEST are noninvasive grading of tumor heterogeneity,[37] determination of the histopathologic malignancy grade, differentiation between therapy effects, and true progression and noninvasive differentiation of 1p/19q codeletion, IDH-and MGMT methylation status.[38-42]

Functional and diffusion tensor imaging

Blood oxygenation level dependent (BOLD)-fMRI is used since more than two decades to measure the hemodynamic response related to a given stimulus related to motor or sensory function, language or memory processing, or visual input The BOLD signal is sensitive to dephasing of the T2* signal and the contrast generated by relative changes in hemoglobin concentrations as an *indirect* consequence of information processing. The BOLD signal is a mixed signal sensitive to blood flow, oxygen concentration and blood volume and strongly correlated with the local field potential, a composite measure that reflects primarily the flow of

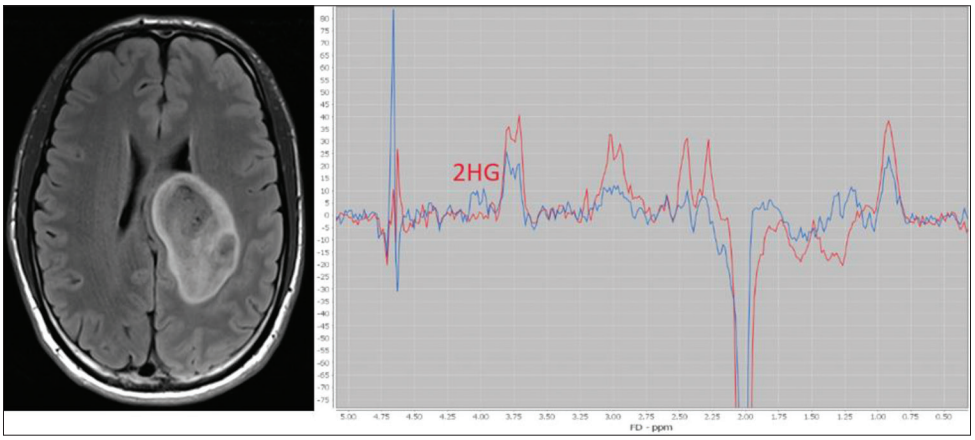

Figure 4: 2-hydroxyglutarate-edited MEGA-semi-LASER spectroscopy (CMRR, TE 60ms) in a patient with a Grade II isocitrate dehydrogenase mutated glioma. The 2-HG multiplet is visible at 4.02 ppm (Courtesy of Prof. J. Slotboom, Bern, with permission)

information across neural networks. Since the BOLD signal receives contributions from multiple neural sources, factors such as regional increases in CBV, low cortical blood volume, and distance between BOLD activations and the tumor are potential confounders that may generate false positive results. A recent meta-analysis that investigated the sensitivity and sensitivity of fMRI reported a sensitivity of 92% and specificity of 76% for motor and of 80% and 71.5% for language protocols in comparison to direct electrical stimulation (DCS).[43] Another study reported a sensitivity of 40% and specificity of 80% on a per patient basis for language mapping in comparison with DCS. Thus, the primarily goal of investigations of the language network is still the determination of the hemispheric dominance. In daily practice, BOLD fMRI is complemented by diffusion tensor imaging, a method that enables structural analysis of structural connectivity between eloquent brain areas by calculating directional diffusivity of water molecules in the white matter. Its principal advantage is the independence from patient compliance and its robustness in acquisition [Figure 6].[44]

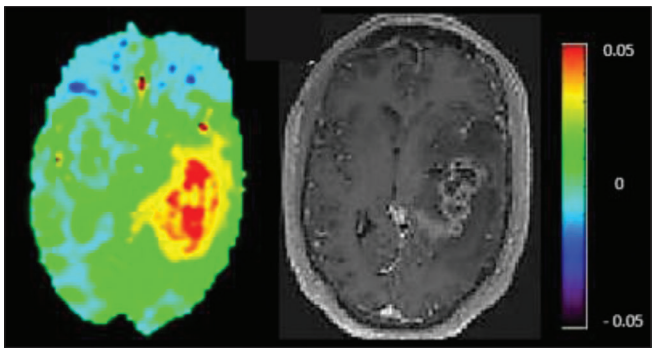

Figure 5: Amide proton transfer-chemical exchange saturation transfer (MTRasym map, left) of a patient with an Grade 4 glioma (GBM). In the GBM, the concentration of proteins is elevated compared to surrounding tissues. The increased intracellular exchanges lead to an increased Amide proton transfer level (Courtesy of Prof Zaiss, Erlangen, with permission)

ULTRA-HIGH FIELD MAGNETIC RESONANCE IMAGING

Clinical ultra-high field (UHF) MRI has recently become feasible with the clearance of 7 T MRI. Currently approximately fifty systems with the FDA 510(k) clearance are available for clinical use worldwide. For glioma imaging, the principal advantages encompass higher spatial resolution due to improved signal to noise and consequently, more detailed information about tumor invasion and tumor vascularization [Figure 7]. Optimizations of RF pulses, parallel and 3D-sequences enable sufficient accelerations of clinical MRI protocols. MRS profits from improvement in spatial and enhanced spectral resolution and identification of metabolites with low concentration, such as glutamate, myo-inositol or 2-hydroxyglutarate.[45,46] In a survey of comparisons between UHF MRI and routine field strength, image quality was improved in 24/51 or noninferior in 17/51 (who were equivalent at both feld strengths), and 9/51 performed less well at UHF MRI.[47]

Image postprocessing

Recently, advances in medical image processing have been achieved through the implementation of artificial intelligence to solve problems associated with extensive time consumption or rater-dependent biases in the detection of tumor volume and of associations between genotype and imaging phenotype. Automated image segmentation enables classification of previously trained tissue categories (e.g., edema, necrosis, enhancing, and nonenhancing tumor) from routinely acquired input images [Figure 8]. The computer is presented with ground truth labels assigned to images to learn the rules that generate the labels of specific tissue classes. The goal of these analyses is to train mainly algorithms based on expert knowledge to achieve the optimal output (i.e. optimal rendering of the posed problem).[48] AI methods have been successfully employed to differentiate genetic mutations[49-51] and regional

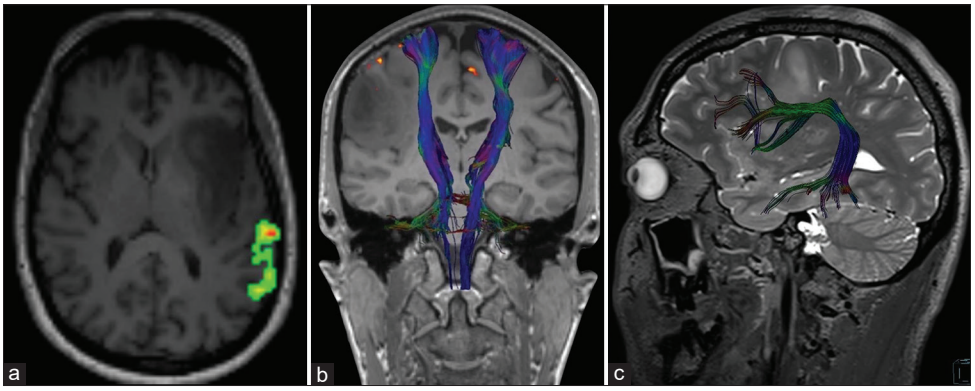

Figure 6: (a) Functional magnetic resonance imaging in a patient with insular glioma. Hemodynamic correlates related to a syntax paradigm (Gutbrod *et al.*, 2012[44]) in the Wernicke area, left hemisphere. (b) Fiber tracking of the corticospinal tract in a patient with LGG. There is a distortion, but no infiltration of the right corticospinal tract. (c) Fiber tracking: Distorted arcuate fascicle in patients with oligodendroglioma

genetic heterogeneity, to define appropriate subregions for biopsy[52,53] or personalized radiotherapy.[54] In addition, automated tumor segmentation can distinguish between tumor-associated edema, tumor necrosis, and enhancing tumor components. For example, neural network-based expert systems are already used to complement visual analysis for glioma volume calculation and calculate tumor volume within a few seconds with an error rate comparable to medical experts.[48,55] In a retrospective analysis in a multicenter dataset from a prospective, randomized phase 2 and 3 trial (EORTC-26101), automated tumor response assessment outperformed RANO assessments for predicting overall survival.[56] By radiomic image analysis, structures within the segmented tumor matrix can be identified that contain prognostically relevant features which represent tumor heterogeneity at a molecular level.[51] For this purpose, correlation tests between quantitative features such as shape, signal distribution, and textures are performed to provide statistical information on malignancy grade, therapy response, and disease progression.[57] Initial retrospective studies demonstrate predictive value for progression-free survival and overall survival of glioma patients independent of clinical and molecular markers. However, the analyses are sensitive to image protocols. Still, many derived features are lacking robustness in multi-center data and are sensitive to bias

Impact on patient management

Differential diagnosis

Due to differences in microvascular and molecular biology in different tumor entities and between neoplastic and nonneoplastic lesions, advanced imaging can be used to differentiate these lesions[58]e.g., glioblastoma multiforme (GBM) versus a brain abscess or vs. tumefactive demyelinating lesion[59,60] CBV values are higher in patients with GBM than in patients with a brain abscess or an inflammatory[61] or tumefactive lesion [Figure 9].[62] It also helps to discriminate different neoplastic lesions (such as the differentiation between GBM, metastasis, and lymphoma).[63-65]

Moreover, peritumoral infiltration can be detected with advanced imaging by increased CBV, AUC, K_{trans} or increase in Cho/Cr or Cho/NAA ratios in areas of T2 hyperintensity adjacent to the contrast-enhancing lesion.[64,66-68] Peritumoral perfusion or metabolic abnormalities are absent in lymphoma or metastasis [Figure 10]. However, accuracy is moderate for differentiating high-grade glioma from lymphoma.[69]

Treatment planning

Glioma grading

Histological and molecular analysis is the gold standard for glioma grading. However, it is an invasive procedure, and in

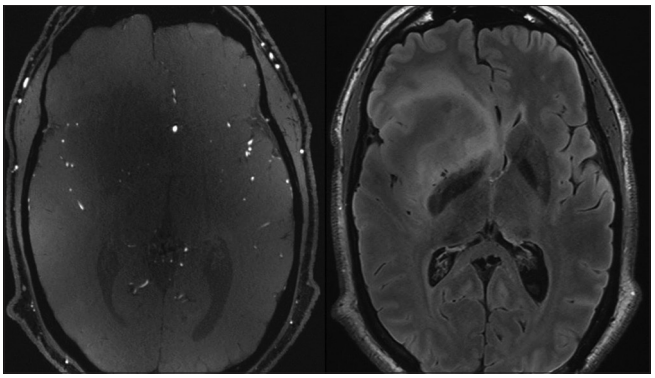

Figure 7: Ultra-high field magnetic resonance imaging: ToF and 3-D FLAIR sequence show the regional vascularization and extension of a right frontal LGG

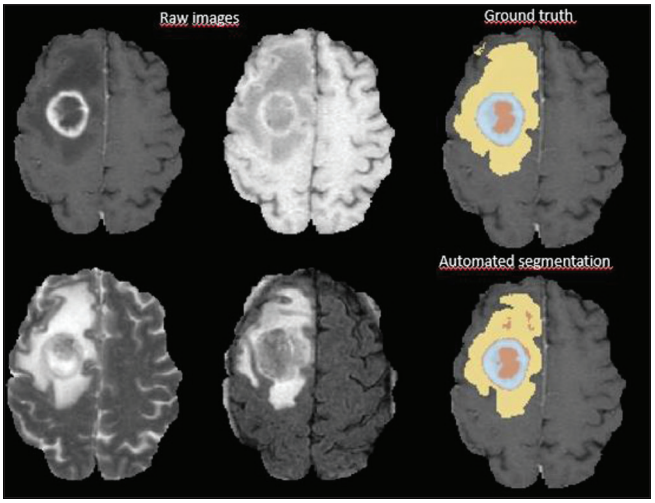

Figure 8: Segmentation results of an automated brain tumor segmentation in a GBM. Enhancing component of the tumor (cyan), necrotic part of the tumor (orange), vasogenic edema (yellow) are seen

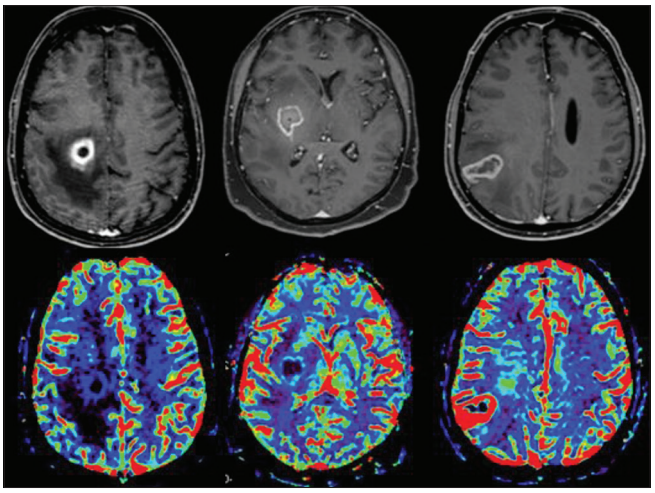

Figure 9: Dynamic susceptibility contrast perfusion maps of a patient with brain abscess, high-grade glioma and lymphoma, respectively. The contrast enhancing rim of the brain abscess is ill-perfused, while the enhancing part of the high-grade glioma shows severly increased Relative cerebral blood volume. In lymphoma, the Relative cerebral blood volume is slightly elevated

some instances, the patient is not eligible for surgery or the tumor's localization restricts resection [Figure 11]. Relying on conventional imaging for tumor grading is not accurate, as low-grade gliomas can show contrast enhancement and high-grade gliomas may not enhance.[70,71] In these instances, advanced imaging can provide a "second reference" for tumor grading. DCE maps (v_e and v_p), as well as DSC map (CBV) have high accuracy for glioma grading.[3] DCE has high accuracy in differentiating between high-grade and low-grade gliomas.[69]

Low-grade gliomas show lower CBV values than high-grade gliomas [Figure 12]. CBV is associated with increased mitotic activity and vascularity.[72,73] Oligodendrogliomas frequently show higher CBV values than diffuse astrocytomas of similar histological grade.[74]

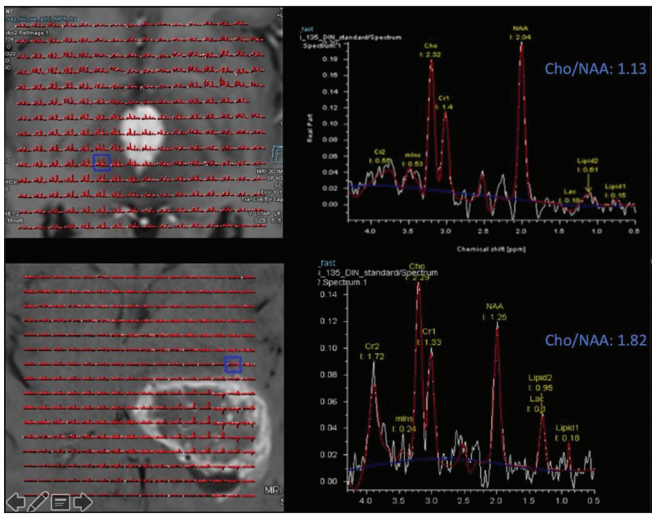

Figure 10: Magnetic resonance spectroscopy from two different patients. Upper row: Patient with lymphoma and normal peritumoral spectra and a Cho/NAA ratio of 1.1. Lower row: Patient with GBM and increased peritumoral Cho/NAA ratio of 1.8

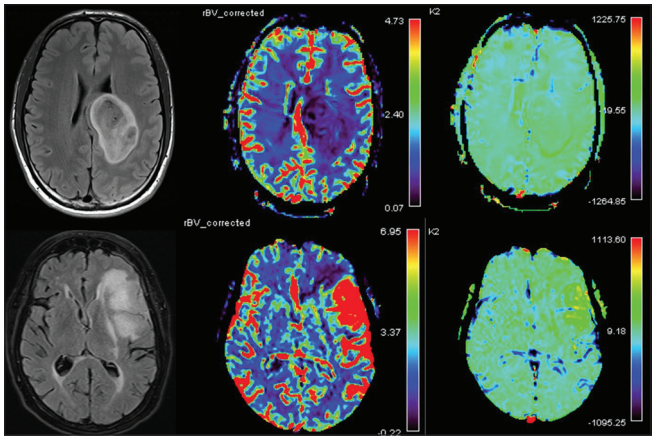

Figure 12: Relative cerebral blood volume differences in a LGG versus a high-grade glioma. Axial FLAIR (left), relative cerebral blood volume (midlle) and leakage (K2) maps of two patients with gliomas. Upper row: WHO II isocitrate dehydrogenase mutated glioma with decreased relative cerebral blood volume without leakage. Lower row: WHO IV isocitrate dehydrogenase mutated tumor with increased relative cerebral blood volume and increased leakage

Outcome prediction

Tumors with higher CBV values at baseline have a shorter time to progression or death than tumors with lower CBV values.[73,75,76] Therefore, tumors showing higher CBV values, even with low histological grade should be treated more aggressively than tumors with lower CBV.[16] CBV values in astrocytomas outperformed histopathological grading as predictor for recurrence and 1-year survival.[77,78] Increased v_e predicts worse progression-free survival and overall survival in patients with high-grade gliomas.[79]

Sampling errors

Due to the internal heterogeneous nature of gliomas, biopsies are prone to sampling errors and underestimation of tumor grading. Advanced imaging can guide the planning of the biopsy. As CBV is a marker for neoangiogenesis and Choline is a marker of mitotic activity, both can be used to identify the tumors area of highest grade[80] [Figure 13].

Follow-up

Adding advanced imaging to the conventional MRI protocol in the follow-up of low-grade gliomas allows for

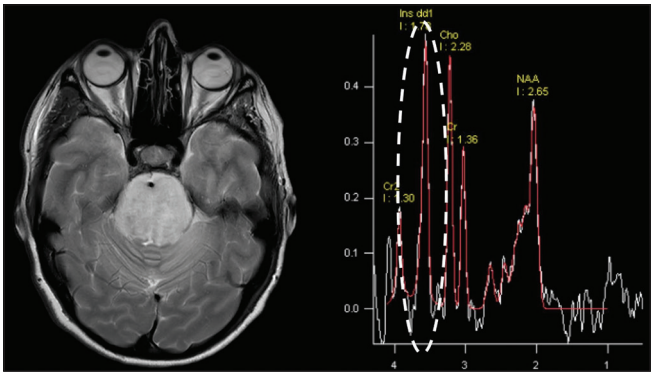

Figure 11: Magnetic resonance spectroscopy of a patient with a diffuse brain stem glioma: The elevated myo-insositol peak is indicative for a LGG: No biopsy was performed due to the localization of the tumor

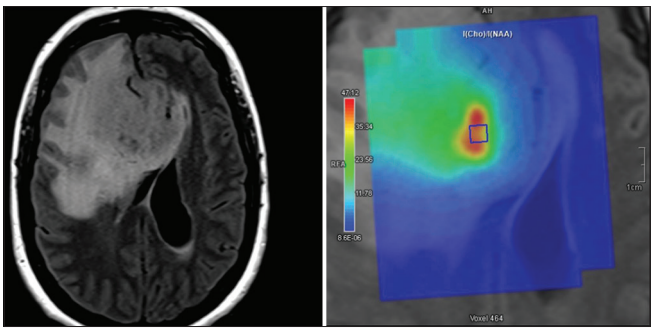

Figure 13: Magnetic resonance spectroscopy for image-guided biopsy. The focally increased Cho/NAA ratio is indicative of the higher tumor grade and should be the target of the biopsy

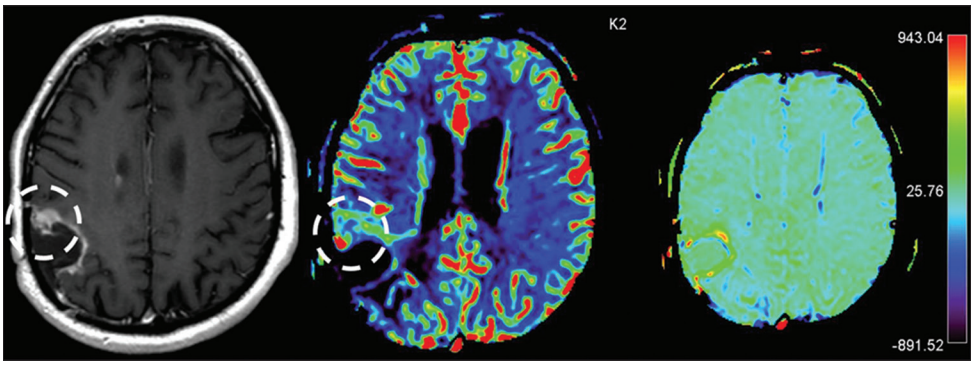

Figure 14: Differentiation between tumor recurrence and radiation necrosis. Tumor recurrence in a 68-year-old male patient after resection and radiotherapy for GBM. Axial contrast enhancing T1 showing nodular enhancement (circle). Cerebral blood volume showing increased perfusion, indicative of a recurrent tumor (histologically proven)

the early detection of malignant transformation.[81] The criteria for assessment of tumor response under therapy are based on measuring the enhancing lesion and evaluation of the T2 changes; however, treatment with chemoradiotherapy causes similar changes to neoplastic changes on conventional imaging,[82] due to vasodilatation, edema, and demyelination after treatment.[9,16] Therefore, the term 'pseudoprogression' has been coined[83,84] as these imaging findings cannot easily be differentiated from true tumor progression. Advanced imaging can address this limitation, as these images address the vascularity and metabolism of tumors which differs from radiation-induced changes.[85,86] True progression shows higher CBV values than radiation-induced changes[19,87-90] [Figure 14]. Parameters reflecting blood volume (CBV, AUC)[91] and permeability derived parameters[92] or v_e[93] as well as MRS,[94] are helpful in this differentiation. In a systematic comparison of DSC and DCE, both methods were equivalent in the discrimination between tumor tissue and therapy-related effects[89] and outperform the RANO criteria that are solely depending on conventional imaging interpretations.[95] Similarly, using perfusion imaging can differentiate between recurrent metastasis and radiation necrosis.[96]

Patients under therapy with angiogenesis inhibitors (e.g. Bevacizumab) may present with decreased or absent tumor enhancement in the follow-up with stationary or increased tumor volume. This contrast reduction is a consequence of a reduced leakage in the tumor vascular bed.[84] This phenomenon is called pseudoresponse[82] and can be mistaken as a true response when using conventional MRI imaging [Figure 15]. MR perfusion and spectroscopy support the discrimination of these entities.

CONCLUSION

The ongoing development of neuro-oncological imaging aims at the detection of cerebral gliomas and the differentiation of therapy-associated changes from tumor progression, furthermore at the prognosis assessment under therapy. Advanced neuroimaging and automated image analysis techniques are used for this purpose. This creates new interdisciplinary challenges and professional profiles in imaging, for which close collaboration between neuropathologists, engineers, image informatics experts and radiologists is indispensable.

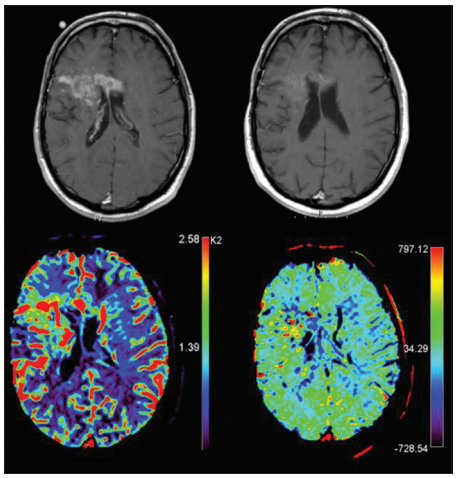

Figure 15: Dynamic susceptibility contrast perfusion imaging. Pseudoresponse: Recurrent GBM under Bevacizumab. Despite radiographic response on the contrast-enhanced T1w image (upper row), there is a persistence of elevated relative cerebral blood volume and increased leakage indicating pseudoprogression

Financial support and sponsorship

Nil.

Conflicts of interest

There are no conflicts of interest.

REFERENCES

1. Ellingson BM, Bendszus M, Boxerman J, Barboriak D, Erickson BJ, Smits M, *et al.* Consensus recommendations for a standardized Brain Tumor Imaging Protocol in clinical trials. Neuro Oncol

2015;17:1188-98.
2. Ellingson BM, Wen PY, Cloughesy TF. Modified criteria for radiographic response assessment in glioblastoma clinical trials. Neurotherapeutics 2017;14:307-20.
3. Young RJ, Gupta A, Shah AD, Graber JJ, Zhang Z, Shi W, *et al.* Potential utility of conventional MRI signs in diagnosing pseudoprogression in glioblastoma. Neurology 2011;76:1918-24.
4. Thust SC, Heiland S, Falini A, Jäger HR, Waldman AD, Sundgren PC, *et al.* Glioma imaging in Europe: A survey of 220 centres and recommendations for best clinical practice. Eur Radiol 2018;28:3306-17.
5. Artzi M, Liberman G, Nadav G, Vitinshtein F, Blumenthal DT, Bokstein F, *et al.* Human cerebral blood volume measurements using dynamic contrast enhancement in comparison to dynamic susceptibility contrast MRI. Neuroradiology 2015;57:671-8.
6. Tofts PS, Kermode AG. Measurement of the blood-brain barrier permeability and leakage space using dynamic MR imaging. 1. Fundamental concepts. Magn Reson Med 1991;17:357-67.
7. Tofts PS. Modeling tracer kinetics in dynamic Gd-DTPA MR imaging. J Magn Reson Imaging 1997;7:91-101.
8. Tofts PS, Brix G, Buckley DL, Evelhoch JL, Henderson E, Knopp MV, *et al.* Estimating kinetic parameters from dynamic contrast-enhanced t1-weighted MRI of a diffusable tracer: Standardized quantities and symbols. J Magn Reson Imaging 1999;10:223-32.
9. van Dijken BRJ, van Laar PJ, Smits M, Dankbaar JW, Enting RH, van der Hoorn A. Perfusion MRI in treatment evaluation of glioblastomas: Clinical relevance of current and future techniques. J Magn Reson Imaging 2019;49:11-22.
10. Zhang J, Liu H, Tong H, Wang S, Yang Y, Liu G, *et al.* Clinical applications of contrast-enhanced perfusion MRI techniques in gliomas: Recent advances and current challenges. Contrast Media Mol Imaging 2017;2017:7064120.
11. Cha S, Knopp EA, Johnson G, Wetzel SG, Litt AW, Zagzag D. Intracranial mass lesions: Dynamic contrast-enhanced susceptibility-weighted echo-planar perfusion MR imaging. Radiology 2002;223:11-29.
12. Donahue KM, Krouwer HG, Rand SD, Pathak AP, Marszalkowski CS, Censky SC, *et al.* Utility of simultaneously acquired gradient-echo and spin-echo cerebral blood volume and morphology maps in brain tumor patients. Magn Reson Med 2000;43:845-53.
13. Quarles CC, Ward BD, Schmainda KM. Improving the reliability of obtaining tumor hemodynamic parameters in the presence of contrast agent extravasation. Magn Reson Med 2005;53:1307-16.
14. Schmainda KM, Rand SD, Joseph AM, Lund R, Ward BD, Pathak AP, *et al.* Characterization of a first-pass gradient-echo spin-echo method to predict brain tumor grade and angiogenesis. AJNR Am J Neuroradiol 2004;25:1524-32.
15. Boxerman JL, Schmainda KM, Weisskoff RM. Relative cerebral blood volume maps corrected for contrast agent extravasation significantly correlate with glioma tumor grade, whereas uncorrected maps do not. AJNR Am J Neuroradiol 2006;27:859-67.
16. Fallatah S, Golay X, Jäger R, Bisdas S. Dynamic Susceptibility Contrast MRI in Gliomas: What the Radiologist Needs to Know. Hell J Radio 2016;1:56-78.
17. Boxerman JL, Quarles CC, Hu LS, Erickson BJ, Gerstner ER, Smits M, *et al.* Consensus recommendations for a dynamic susceptibility contrast MRI protocol for use in high-grade gliomas. Neuro Oncol 2020;22:1262-75.
18. Jain RK, di Tomaso E, Duda DG, Loeffler JS, Sorensen AG, Batchelor TT. Angiogenesis in brain tumours. Nat Rev Neurosci 2007;8:610-22.
19. Hu LS, Baxter LC, Smith KA, Feuerstein BG, Karis JP, Eschbacher JM, *et al.* Relative cerebral blood volume values to differentiate high-grade glioma recurrence from posttreatment radiation effect: Direct correlation between image-guided tissue histopathology and localized dynamic susceptibility-weighted contrast-enhanced perfusion MR imaging measurements. AJNR Am J Neuroradiol 2009;30:552-8.
20. Cha S, Johnson G, Wadghiri YZ, Jin O, Babb J, Zagzag D, *et al.* Dynamic, contrast-enhanced perfusion MRI in mouse gliomas: Correlation with histopathology. Magn Reson Med 2003;49:848-55.
21. Jain R, Gutierrez J, Narang J, Scarpace L, Schultz LR, Lemke N, *et al. In vivo* correlation of tumor blood volume and permeability with histologic and molecular angiogenic markers in gliomas. AJNR Am J Neuroradiol 2011;32:388-94.
22. Anzalone N, Castellano A, Cadioli M, Conte GM, Cuccarini V, Bizzi A, *et al.* Brain gliomas: Multicenter standardized assessment of dynamic contrast-enhanced and dynamic susceptibility contrast MR images. Radiology 2018;287:933-43.
23. Federau C, Meuli R, O'Brien K, Maeder P, Hagmann P. Perfusion measurement in brain gliomas with intravoxel incoherent motion MRI. AJNR Am J Neuroradiol 2014;35:256-62.
24. Hashido T, Saito S, Ishida T. A radiomics-based comparative study on arterial spin labeling and dynamic susceptibility contrast perfusion-weighted imaging in gliomas. Sci Rep 2020;10:6121.
25. Han S, Liu Y, Cai SJ, Qian M, Ding J, Larion M, *et al.* IDH mutation in glioma: Molecular mechanisms and potential therapeutic targets. Br J Cancer 2020;122:1580-9.
26. Smits M, van den Bent MJ. Imaging correlates of adult glioma genotypes. Radiology 2017;284:316-31.
27. Ellingson BM, Lai A, Harris RJ, Selfridge JM, Yong WH, Das K, *et al.* Probabilistic radiographic atlas of glioblastoma phenotypes. AJNR Am J Neuroradiol 2013;34:533-40.
28. Kickingereder P, Sahm F, Radbruch A, Wick W, Heiland S, Deimling Av, *et al.* IDH mutation status is associated with a distinct hypoxia/angiogenesis transcriptome signature which is non-invasively predictable with rCBV imaging in human glioma. Sci Rep 2015;5:16238.
29. Suh CH, Kim HS, Jung SC, Choi CG, Kim SJ. Clinically relevant imaging features for MGMT promoter methylation in multiple glioblastoma studies: A systematic review and meta-analysis. Am J Neuroradiol 2018;39:1439-45.
30. Öz G, Alger JR, Barker PB, Bartha R, Bizzi A, Boesch C, *et al.* Clinical proton MR spectroscopy in central nervous system disorders. Radiology 2014;270:658-79.
31. Andronesi OC, Kim GS, Gerstner E, Batchelor T, Tzika AA, Fantin VR, *et al.* Detection of 2-hydroxyglutarate in IDH-mutated glioma patients by *in vivo* spectral-editing and 2D correlation magnetic resonance spectroscopy. Sci Transl Med 2012;4:116ra4.
32. Choi C, Ganji SK, DeBerardinis RJ, Hatanpaa KJ, Rakheja D, Kovacs Z, *et al.* 2-Hydroxyglutarate detection by magnetic resonance spectroscopy in IDH-mutated patients with gliomas. Nat Med 2012;18:624-9.
33. Zhou M, Zhou Y, Liao H, Rowland BC, Kong X, Arvold ND, *et al.* Diagnostic accuracy of 2-hydroxyglutarate magnetic resonance spectroscopy in newly diagnosed brain mass and suspected recurrent gliomas. Neuro Oncol 2018;20:1262-71.
34. Suh CH, Kim HS, Jung SC, Choi CG, Kim SJ. 2-Hydroxyglutarate MR spectroscopy for prediction of isocitrate dehydrogenase mutant glioma: A systemic review and meta-analysis using individual patient data. Neuro Oncol 2018;20:1573-83.
35. Zhou J, van Zijl PC. Chemical exchange saturation transfer imaging and spectroscopy. Prog Nucl Magn Reson Spectrosc 2006;48:109-36.
36. Zhou J, Lal B, Wilson DA, Laterra J, van Zijl PC. Amide proton transfer (APT) contrast for imaging of brain tumors. Magn Reson Med 2003;50:1120-6.
37. Warnert EAH, Wood TC, Incekara F, Barker GJ, Vincent AJP, Schouten J, *et al.* Mapping tumour heterogeneity with pulsed 3D CEST MRI in non-enhancing glioma at 3 T. MAGMA 2021: doi 10.1007/s10334-021-00911-6.
38. Jiang S, Zou T, Eberhart CG, Villalobos MAV, Heo HY, Zhang Y, *et al.* Predicting IDH mutation status in grade II gliomas using amide proton transfer-weighted (APTw) MRI. Magn Reson Med 2017;78:1100-9.
39. Kamimura K, Nakajo M, Yoneyama T, Takumi K, Kumagae Y, Fukukura Y, *et al.* Amide proton transfer imaging of tumors: Theory, clinical applications, pitfalls, and future directions. Jpn J Radiol 2019;37:109-16.

40. Zhou J, Heo HY, Knutsson L, van Zijl PCM, Jiang S. APT-weighted MRI: Techniques, current neuro applications, and challenging issues. J Magn Reson Imaging 2019;50:347-64.
41. Yao J, Chakhoyan A, Nathanson DA, Yong WH, Salamon N, Raymond C, *et al.* Metabolic characterization of human IDH mutant and wild type gliomas using simultaneous pH- and oxygen-sensitive molecular MRI. Neuro Oncol 2019;21:1184-96.
42. Yao J, Hagiwara A, Raymond C, Shabani S, Pope WB, Salamon N, *et al.* Human IDH mutant 1p/19q co-deleted gliomas have low tumor acidity as evidenced by molecular MRI and PET: A retrospective study. Sci Rep 2020;10:11922.
43. Metwali H, Raemaekers M, Kniese K, Kardavani B, Fahlbusch R, Samii A. Reliability of functional magnetic resonance imaging in patients with brain tumors: A critical review and meta-analysis. World Neurosurg 2019;125:183-90.
44. Gutbrod K, Spring D, Degonda N, Heinemann D, Nirkko A, Hauf M, *et al.* Determination of language dominance: Wada test and fMRI compared using a novel sentence task. J Neuroimaging 2012;22:266-74.
45. Verma G, Mohan S, Nasrallah MP, Brem S, Lee JY, Chawla S, *et al.* Non-invasive detection of 2-hydroxyglutarate in IDH-mutated gliomas using two-dimensional localized correlation spectroscopy (2D L-COSY) at 7 Tesla. J Transl Med 2016;14:274.
46. Lupo JM, Li Y, Hess CP, Nelson SJ. Advances in ultra-high field MRI for the clinical management of patients with brain tumors. Curr Opin Neurol 2011;24:605-15.
47. Barrett TF, Sarkiss CA, Dyvorne HA, Lee J, Balchandani P, Shrivastava RK. Application of ultrahigh field magnetic resonance imaging in the treatment of brain tumors: A meta-analysis. World Neurosurg 2016;86:450-65.
48. Rebsamen M, Knecht U, Reyes M, Wiest R, Meier R, McKinley R. Divide and conquer: Stratifying training data by tumor grade improves deep learning-based brain tumor segmentation. Front Neurosci 2019;13:1182.
49. Chang P, Grinband J, Weinberg BD, Bardis M, Khy M, Cadena G, *et al.* Deep-learning convolutional neural networks accurately classify genetic mutations in gliomas. AJNR Am J Neuroradiol 2018;39:1201-7.
50. Eichinger P, Alberts E, Delbridge C, Trebeschi S, Valentinitsch A, Bette S, *et al.* Diffusion tensor image features predict IDH genotype in newly diagnosed WHO grade II/III gliomas. Sci Rep 2017;7:13396.
51. Hu LS, Ning S, Eschbacher JM, Baxter LC, Gaw N, Ranjbar S, *et al.* Radiogenomics to characterize regional genetic heterogeneity in glioblastoma. Neuro Oncol 2017;19:128-37.
52. Chang PD, Malone HR, Bowden SG, Chow DS, Gill BJA, Ung TH, *et al.* A multiparametric model for mapping cellularity in glioblastoma using radiographically localized biopsies. AJNR Am J Neuroradiol 2017;38:890-8.
53. Menze BH, Van Leemput K, Honkela A, Konukoglu E, Weber MA, Ayache N, *et al.* A generative approach for image-based modeling of tumor growth. Inf Process Med Imaging 2011;22:735-47.
54. Lipkova J, Angelikopoulos P, Wu S, Alberts E, Wiestler B, Diehl C, *et al.* Personalized radiotherapy design for glioblastoma: Integrating mathematical tumor models, multimodal scans, and bayesian inference. IEEE Trans Med Imaging 2019;38:1875-84.
55. Rebsamen M, Suter Y, Wiest R, Reyes M, Rummel C. Brain morphometry estimation: From hours to seconds using deep learning. Front Neurol 2020;11:244.
56. Kickingereder P, Isensee F, Tursunova I, Petersen J, Neuberger U, Bonekamp D, *et al.* Automated quantitative tumour response assessment of MRI in neuro-oncology with artificial neural networks: A multicentre, retrospective study. Lancet Oncol 2019;20:728-40.
57. Soni N, Priya S, Bathla G. Texture analysis in cerebral gliomas: A review of the literature. AJNR Am J Neuroradiol 2019;40:928-34.
58. Hourani R, Brant LJ, Rizk T, Weingart JD, Barker PB, Horská A. Can proton MR spectroscopic and perfusion imaging differentiate between neoplastic and nonneoplastic brain lesions in adults? AJNR Am J Neuroradiol 2008;29:366-72.
59. Toh CH, Wei KC, Chang CN, Ng SH, Wong HF, Lin CP. Differentiation of brain abscesses from glioblastomas and metastatic brain tumors: Comparisons of diagnostic performance of dynamic susceptibility contrast-enhanced perfusion MR imaging before and after mathematic contrast leakage correction. PLoS One 2014;9:e109172.
60. Holmes TM, Petrella JR, Provenzale JM. Distinction between cerebral abscesses and high-grade neoplasms by dynamic susceptibility contrast perfusion MRI. AJR Am J Roentgenol 2004;183:1247-52.
61. Floriano VH, Torres US, Spotti AR, Ferraz-Filho JR, Tognola WA. The role of dynamic susceptibility contrast-enhanced perfusion MR imaging in differentiating between infectious and neoplastic focal brain lesions: Results from a cohort of 100 consecutive patients. PLoS One 2013;8:e81509.
62. Cha S, Pierce S, Knopp EA, Johnson G, Yang C, Ton A, *et al.* Dynamic contrast-enhanced T2*-weighted MR imaging of tumefactive demyelinating lesions. AJNR Am J Neuroradiol 2001;22:1109-116.
63. Hakyemez B, Erdogan C, Bolca N, Yildirim N, Gokalp G, Parlak M. Evaluation of different cerebral mass lesions by perfusion-weighted MR imaging. J Magn Reson Imaging 2006;24:817-24.
64. Neska-Matuszewska M, Bladowska J, Sąsiadek M, Zimny A. Differentiation of glioblastoma multiforme, metastases and primary central nervous system lymphomas using multiparametric perfusion and diffusion MR imaging of a tumor core and a peritumoral zone-Searching for a practical approach. PLoS One 2018;13:e0191341.
65. Weber MA, Zoubaa S, Schlieter M, Juttler E, Huttner HB, Geletneky K, *et al.* Diagnostic performance of spectroscopic and perfusion MRI for distinction of brain tumors. Neurology 2006;66:1899-906.
66. Law M, Cha S, Knopp EA, Johnson G, Arnett J, Litt AW. High-grade gliomas and solitary metastases: Differentiation by using perfusion and proton spectroscopic MR imaging. Radiology 2002;222:715-21.
67. Tupý R, Mírka H, Mraček J, Přibáň V, Hes O, Vokurka S, *et al.* Tumor-related perfusion changes in white matter adjacent to brain tumors: Pharmacodynamic analysis of dynamic 3T magnetic resonance imaging. Anticancer Res 2018;38:4149-52.
68. Zhao J, Yang ZY, Luo BN, Yang JY, Chu JP. Quantitative evaluation of diffusion and dynamic contrast-enhanced MR in tumor parenchyma and peritumoral area for distinction of brain tumors. PLoS One 2015;10:e0138573.
69. Okuchi S, Rojas-Garcia A, Ulyte A, Lopez I, Ušinskienė J, Lewis M, *et al.* Diagnostic accuracy of dynamic contrast-enhanced perfusion MRI in stratifying gliomas: A systematic review and meta-analysis. Cancer Med 2019;8:5564-73.
70. Scott JN, Brasher PMA, Sevick RJ, Rewcastle NB, Forsyth PA. How often are nonenhancing supratentorial gliomas malignant? A population study. Neurology 2002;59:947-9.
71. Barker FG 2nd, Chang SM, Huhn SL, Davis RL, Gutin PH, McDermott MW, *et al.* Age and the risk of anaplasia in magnetic resonance-nonenhancing supratentorial cerebral tumors. Cancer 1997;80:936-41.
72. Aronen HJ, Gazit IE, Louis DN, Buchbinder BR, Pardo FS, Weisskoff RM, *et al.* Cerebral blood volume maps of gliomas: Comparison with tumor grade and histologic findings. Radiology 1994;191:41-51.
73. Law M, Oh S, Johnson G, Babb JS, Zagzag D, Golfinos J, *et al.* Perfusion magnetic resonance imaging predicts patient outcome as an adjunct to histopathology: A second reference standard in the surgical and nonsurgical treatment of low-grade gliomas. Neurosurgery 2006;58:1099-107.
74. Saito T, Yamasaki F, Kajiwara Y, Abe N, Akiyama Y, Kakuda T, *et al.* Role of perfusion-weighted imaging at 3T in the histopathological differentiation between astrocytic and oligodendroglial tumors. Eur J Radiol 2012;81:1863-9.
75. Law M, Oh S, Babb JS, Wang E, Inglese M, Zagzag D, *et al.* Low-Grade gliomas: Dynamic susceptibility-weighted contrast-enhanced perfusion MR imaging – Prediction of patient clinical response. Radiology 2006;238:658-67.
76. Caseiras GB, Chheang S, Babb J, Rees JH, Pecerrelli N, Tozer DJ, *et al.*

Relative cerebral blood volume measurements of low-grade gliomas predict patient outcome in a multi-institution setting. Eur J Radiol 2010;73:215-20.
77. Bisdas S, Kirkpatrick M, Giglio P, Welsh C, Spampinato MV, Rumboldt Z. Cerebral blood volume measurements by perfusion-weighted MR imaging in gliomas: Ready for prime time in predicting short-term outcome and recurrent disease? AJNR Am J Neuroradiol 2009;30:681-8.
78. Bag AK, Cezayirli PC, Davenport JJ, Gaddikeri S, Fathallah-Shaykh HM, Cantor A, *et al.* Survival analysis in patients with newly diagnosed primary glioblastoma multiforme using pre- and post-treatment peritumoral perfusion imaging parameters. J Neurooncol 2014;120:361-70.
79. Ulyte A, Katsaros VK, Liouta E, Stranjalis G, Boskos C, Papanikolaou N, *et al.* Prognostic value of preoperative dynamic contrast-enhanced MRI perfusion parameters for high-grade glioma patients. Neuroradiology 2016;58:1197-208.
80. Maia AC Jr., Malheiros SM, da Rocha AJ, Stávale JN, Guimarães IF, Borges LR, *et al.* Stereotactic biopsy guidance in adults with supratentorial nonenhancing gliomas: Role of perfusion-weighted magnetic resonance imaging. J Neurosurg 2004;101:970-6.
81. Danchaivijitr N, Waldman AD, Tozer DJ, Benton CE, Brasil Caseiras G, Tofts PS, *et al.* Low-grade gliomas: Do changes in rCBV measurements at longitudinal perfusion-weighted MR imaging predict malignant transformation? Radiology 2008;247:170-8.
82. Fu F, Sun X, Li Y, Liu Y, Shan Y, Ji N, *et al.* Dynamic contrast-enhanced magnetic resonance imaging biomarkers predict chemotherapeutic responses and survival in primary central-nervous-system lymphoma. Eur Radiol 2021;31:1863-71.
83. Brandsma D, Stalpers L, Taal W, Sminia P, van den Bent MJ. Clinical features, mechanisms, and management of pseudoprogression in malignant gliomas. Lancet Oncol 2008;9:453-61.
84. Hygino da Cruz LC Jr., Rodriguez I, Domingues RC, Gasparetto EL, Sorensen AG. Pseudoprogression and pseudoresponse: Imaging challenges in the assessment of posttreatment glioma. AJNR Am J Neuroradiol 2011;32:1978-85.
85. Prah MA, Al-Gizawiy MM, Mueller WM, Cochran EJ, Hoffmann RG, Connelly JM, *et al.* Spatial discrimination of glioblastoma and treatment effect with histologically-validated perfusion and diffusion magnetic resonance imaging metrics. J Neurooncol 2018;136:13-21.
86. Hoxworth JM, Eschbacher JM, Gonzales AC, Singleton KW, Leon GD, Smith KA, *et al.* Performance of standardized relative CBV for quantifying regional histologic tumor burden in recurrent high-grade glioma: Comparison against Normalized relative CBV using image-localized stereotactic biopsies. AJNR Am J Neuroradiol 2020;41:408-15.
87. Young RJ, Gupta A, Shah AD, Graber JJ, Chan TA, Zhang Z, *et al.* MRI perfusion in determining pseudoprogression in patients with glioblastoma. Clin Imaging 2013;37:41-9.
88. Xu JL, Shi DP, Dou SW, Li YL, Yan FS. Distinction between postoperative recurrent glioma and delayed radiation injury using MR perfusion weighted imaging. J Med Imaging Radiat Oncol 2011;55:587-94.
89. Patel P, Baradaran H, Delgado D, Askin G, Christos P, John Tsiouris A, *et al.* MR perfusion-weighted imaging in the evaluation of high-grade gliomas after treatment: A systematic review and meta-analysis. Neuro Oncol 2017;19:118-27.
90. Larsen VA, Simonsen HJ, Law I, Larsson HB, Hansen AE. Evaluation of dynamic contrast-enhanced T1-weighted perfusion MRI in the differentiation of tumor recurrence from radiation necrosis. Neuroradiology 2013;55:361-9.
91. Zakhari N, Taccone MS, Torres CH, Chakraborty S, Sinclair J, Woulfe J, *et al.* Prospective comparative diagnostic accuracy evaluation of dynamic contrast-enhanced (DCE) vs. dynamic susceptibility contrast (DSC) MR perfusion in differentiating tumor recurrence from radiation necrosis in treated high-grade gliomas. J Magn Reson Imaging 2019;50:573-82.
92. Bisdas S, Naegele T, Ritz R, Dimostheni A, Pfannenberg C, Reimold M, *et al.* Distinguishing recurrent high-grade gliomas from radiation injury: A pilot study using dynamic contrast-enhanced MR imaging. Acad Radiol 2011;18:575-83.
93. Yoo RE, Choi SH, Kim TM, Park CK, Park SH, Won JK, *et al.* Dynamic contrast-enhanced MR imaging in predicting progression of enhancing lesions persisting after standard treatment in glioblastoma patients: A prospective study. Eur Radiol 2017;27:3156-66.
94. van Dijken BRJ, van Laar PJ, Holtman GA, van der Hoorn A. Diagnostic accuracy of magnetic resonance imaging techniques for treatment response evaluation in patients with high-grade glioma, a systematic review and meta-analysis. Eur Radiol 2017;27:4129-44.
95. Batchelor TT, Sorensen AG, di Tomaso E, Zhang WT, Duda DG, Cohen KS, *et al.* AZD2171, a pan-VEGF receptor tyrosine kinase inhibitor, normalizes tumor vasculature and alleviates edema in glioblastoma patients. Cancer Cell 2007;11:83-95.
96. Barajas RF, Chang JS, Sneed PK, Segal MR, McDermott MW, Cha S. Distinguishing recurrent intra-axial metastatic tumor from radiation necrosis following gamma knife radiosurgery using dynamic susceptibility-weighted contrast-enhanced perfusion MR imaging. AJNR Am J Neuroradiol 2009;30:367-72.